5

The biosphere: a global perspective

S.O. Los, C.J. Tucker, A. Anyamba, M. Cherlet, G.J. Collatz,
L. Giglio, F.G. Hall and J.A. Kendall

5.1 INTRODUCTION

Satellite monitoring of land surface vegetation at regional and global scales is the topic of this chapter. The chapter provides an overview of developments during the past 20 years, highlights several applications, and discusses pitfalls in the analysis of multi-year satellite data.

Monitoring of land surface vegetation from satellites at regional and global scales is most commonly used to detect year-to-year variations in vegetation. Variations in vegetation can provide us with estimates of interannual variation in crop yield, movements of desert boundaries, and indications of environmental conditions that are associated with the outbreak of pests and diseases. Some of the variations in vegetation are related to quasi-periodic climate oscillations (e.g. El Niño), others are related to the conversion of land, e.g., from a tropical forest into cropland. All applications require data that are comparable in space and time.

Some of the vegetation processes we study with satellite data are of immediate importance; e.g., detection of failed crops or of environmental conditions that are associated with outbreaks of pests and diseases is essential for policy makers to take appropriate action. Other vegetation processes may have importance for longer time-scales, e.g., long-term monitoring of responses of vegetation to variations in climate could help us understand feedbacks between climate and vegetation and improve projections of the impacts of climate and environmental change.

In this chapter several applications related to global and regional monitoring of vegetation are discussed. Most of these applications are based on NOAA Advanced Very High Resolution Radiometer (AVHRR) or Landsat data. The NOAA and Landsat satellites have been in operation for several decades and from the long records collected by these instruments we can obtain meaningful estimates of variations in land surface vegetation during the past two decades. No other globally comprehensive data series provides us with this unique capability to study vegetation over a comparable period at global scales.

Vegetation monitoring at global and regional scales began with the launch of NOAA-7 in 1981. The AVHRR aboard NOAA-7 collected data from the entire globe at least once during daytime and this provided us with the opportunity to obtain frequent updates of vegetation at regional and global scales. The spatial resolution of the AVHRR is much less than of Landsat, hence the possibility to frequently monitor vegetation conditions comes with a loss of spatial detail.

Both the AVHRR and earlier Landsat scanners were first generation instruments and have flaws in their design. As a result, data are often not spatially

and temporally consistent, even though this is a first requirement for meaningful detection of year-to-year variations in vegetation. Often, this requirement of spatial and temporal consistency of vegetation data was an afterthought in the design of previous satellite remote sensing systems. This chapter will show examples of ways to deal with these issues and to extract meaningful information from corrected data. New satellite missions such as SPOT-VEGETATION, TERRA, and Landsat 7 that have been launched recently are designed specifically for vegetation monitoring and are expected to have fewer data problems as a result.

5.2 HISTORIC OVERVIEW

Remote sensing of vegetation at regional scales began with the launch of the Landsat satellite in the mid-seventies (Chapter 3). Most studies that use Landsat data focus on regions of at most several hundred square kilometers. An example of a Landsat based study over a much larger area is the Large Area Crop Inventory Experiment (LACIE). LACIE was initiated to estimate crop yields in the former Soviet Union and to assess global grain markets more reliably. During LACIE, large amounts of Landsat data were used in combination with statistical sampling techniques and simple crop models to estimate crop production in the US and the former Soviet Union.

Continuous monitoring of vegetation at global scales became possible with the launch of the NOAA satellites in 1981. The NOAA satellites carry the Advanced Very High Resolution Radiometer (AVHRR), which collects data globally at least twice daily, once during daytime and once during the night (Chapter 3). However cloud cover and other atmospheric effects reduce the effective coverage. The NOAA satellite was designed for meteorological applications such as cloud analysis, analysis of sea surface temperatures and snow detection. NOAA-AVHRR data were first used for vegetation monitoring in the early eighties (a selection of early papers is referenced by Tucker 1996). The immediate motivation for this research was an imminent failure of Landsat 3 and its long overdue replacement by Landsat 4. AVHRR channel 1 and 2 data with 1.1 km resolution were combined in the Normalized Difference Vegetation Index (NDVI). Seasonal sums of NDVI were calculated from cloud free data over the growing season. The relationships between seasonal sums of NDVI versus annually accumulated above ground biomass (or crop yield) were similar to relationships established via ground measurements by Tucker (1979). Tucker and co-workers concluded that the AVHRR was suitable for the estimation of vegetation primary production. However, several shortcomings were also noticed: view angle dependent variations appeared in NDVI data, the spectral bandwidth of channels 1 and 2 was too broad, and the time of overpass was thought unsuitable: the 7:30 overpass of NOAA 6 was too early because of low light levels and the 14:30 time of overpass of NOAA 7 was thought too late because of cloud build-up.

The Nile-delta study was repeated for Senegal with NOAA 7 data (Tucker *et al.* 1983, 1985b) and for other parts of the Sahel with similar results (Justice 1986, Prince and Justice 1991). During the first year of the Senegal study Tucker and co-workers were fortunate that most of the AVHRR data were cloud free (Tucker *et al.* 1983). During the second year, cloud contamination, atmospheric effects, and

variations in NDVI with viewing angle limited the usefulness of the data. Several techniques were investigated to reduce these effects and enhance data quality (Kimes *et al.* 1984; Holben 1986). The most suitable technique was to form 10 day, 15 day or monthly NDVI composites by selecting the maximum NDVI for each picture element (pixel) over the period considered. This maximum value compositing technique was implemented by the global inventory, modelling, and monitoring system (GIMMS) group to process AVHRR data into 10-day NDVI composites of Africa in near real-time. The United Nations Food and Agricultural Organization (FAO) started to use these data for famine early warning and desert locust detection (Hielkema 1990).

In 1983, NOAA started processing of the Global Vegetation Index (GVI) data set (Tarpley *et al.* 1984). The availability of the GVI and GIMMS-NDVI data sets prompted a host of new research on the spatial distribution and seasonal dynamics of vegetation over large areas. For example, Tucker *et al.* (1985a) estimated land-cover classes of Africa based on seasonal variations detected in NOAA-AVHRR data. Goward and Dye (1987) studied net primary production in North America. Malingreau *et al.* (1985) detected forest fires in southeast Asia during the 1982 El Niño drought. Helldén *et al.* (1984) studied land degradation in southern Sudan. Tucker *et al.* (1986b) studied the relationship between the annual cycles of NDVI and the seasonal variations in absorption of atmospheric CO_2 by vegetation.

When multi-year NOAA-AVHRR data sets became available, several shortcomings were noticed. These shortcomings are related to both the design of the AVHRR and to external sources. Design related shortcomings include changes in the sensitivity of the visible and near-infrared sensors, inaccuracies in the satellite navigation and a gradual change in the local crossing time of the satellite to later hours during its lifetime. External sources of interference are scattering and absorption of solar radiation by atmospheric constituents, variations in soil reflectance, clouds, and variations in NDVI with illumination angle and viewing angle. Illumination effects, also referred to as satellite drift effects, are noticeable as discontinuities in AVHRR time-series when the data receiving protocol changes from one NOAA platform to the next. Several techniques were developed to account for these inconsistencies. A change in sensitivity of the sensor, or sensor degradation, was corrected by assuming signals from deserts and cloud tops invariant (Rao and Chen 1994; Vermote and Kaufman 1995; Los 1998b). Orbital models were improved to obtain more accurate navigation of the NOAA satellites (Rosborough *et al.* 1994). Corrections were developed for atmospheric effects (Tanré *et al.* 1992; Vermote *et al.* 1995), cloud contamination (Stowe *et al.* 1991; Gutman *et al.* 1994), dependence of surface reflectance on viewing and solar angles (Roujean *et al.* 1992; Sellers *et al.* 1996b) and reflection from soil background (Qi *et al.* 1994). The implementation of some of these corrections is straightforward; others require data from additional sources that cannot be obtained with sufficient accuracy.

Several attempts were made to release corrected, spatially and temporally compatible data to the public. Amongst these data sets are the AVHRR land surface Pathfinder data set (James and Kalluri 1994), the FASIR NDVI data set (Sellers *et al.* 1996b; Los *et al.* 2000) and the 3rd generation GVI data set (Gutman *et al.* 1994). These data sets were developed for different purposes: The Pathfinder data

and GVI data were developed for observational purposes whereas the FASIR NDVI data were designed for use with models.

With the availability of longer NOAA-AVHRR data records, it became possible to study the effects of interannual variations in climate on vegetation. An important source of climate variation is El Niño. El Niño is a warming of the eastern equatorial Pacific Ocean and has been associated with disruptions in rainfall patterns over large areas, especially in the tropics (Skidmore 1988). These disruptions in rainfall result in variations in vegetation and these can be detected from satellite (Myneni *et al.* 1995; Anyamba and Eastman 1996; Los *et al.* 2001). Warming of mid and high northern latitudes leads to earlier springs and this may result in an earlier greening of vegetation, although there is still debate about the accuracy of the reported trend in AVHRR NDVI data (Malmström *et al.* 1997; Myneni *et al.* 1997; Gutman 1999; and Los *et al.* 2000, 2001). A link between El Niño and wild fire activity has also been proven (Skidmore 1988).

Interest in the effects of vegetation on the global carbon balance, water balance and energy balance lead to the development of improved land surface sub-models in climate models and biogeochemical models (Sellers *et al.* 1996b, 1996c, Potter *et al.* 1993; Field *et al.* 1995). Satellite data are used to estimate biophysical parameters in these new land surface models (Sellers *et al.* 1996b, 1996c). Satellite derived biophysical land surface parameters show more realistic spatial and temporal variability than previously prescribed land surface parameters that were estimated from land cover types and look-up tables (Sellers *et al.* 1996b).

Useful information about vegetation cannot only be obtained from visible and near infrared channels, but also from thermal channels. Thermal channels have the ability to detect fires, if these are sufficiently large. Thermal data can thus provide information on timing and location of fires and provide information on the role of wild fires for, e.g. air quality and the carbon cycle. Interest in the study of wild fires renewed when large outbreaks occurred during the El Niño year of 1998.

5.3 LANDSAT BASED REGIONAL STUDIES

Landsat data are used mostly to obtain information of the land surface for a region. They provide a snapshot of a region for a particular time that is used to obtain information on land cover types (see also Chapters 3, 6, 7 and 9 for illustrations of several applications). For some areas two or three useful (e.g. cloud free) snapshots may be available for a particular year, other areas may have less frequent coverage. This low temporal coverage in combination with the large data volumes that need to be handled makes Landsat data less suitable for monitoring of large areas at frequent intervals. Because of the computing resources needed, uncertainties in acquiring data in a timely fashion and the costs involved, few institutions will be able to do high temporal resolution, large area analysis. Two examples follow where Landsat data are used to monitor vegetation over large areas. The first example uses statistical sampling of Landsat data to estimate crop yield in the former Soviet Union. The second example uses Landsat data at about 10-year intervals to estimate the rate of tropical deforestation in the Amazon.

5.3.1 The Large Area Crop Inventory Program

The Large Area Crop Inventory Program (LACIE) was initiated to obtain timely, reliable estimates of crop production for several important wheat exporting countries in the world (MacDonald and Hall 1980). These estimates are often lacking or inadequate because of insufficient funding or limited technical capabilities at the country level. For example, lack of information on a shortfall in grain crop in the former Soviet Union led the US to sell grain at a below-market price in 1972 and 1977. Timely availability of this information could have avoided this negative effect on the US economy.

The LACIE program used Landsat data, meteorological data (monthly mean temperature and rainfall) and ancillary data such as crop maturity calendars, cropping practices, field size, modelled adjustments to the normal wheat crop calendar in response to the current year's weather as well as summaries of the meteorological and crop conditions for the current crop year. Ground-acquired data on crop identification and crop condition were used to develop techniques and assess the accuracy of the LACIE system.

Crop acreage was estimated from stratified random samples of Landsat data with a manually assisted machine processing approach. This sampling was an important step because it reduced the large volumes of Landsat data to be handled. Stratification was based on administrative regions. Within each stratum, sample units were selected consisting of segments of Landsat data of approximately 9 by 11 km. About 2 per cent of the Landsat data were selected at random, which incurs a sampling error of less than 2 per cent. An image analyst used the spatial context in the segments and the phenological stage of vegetation to label about 100 Landsat pixels as small-grain crops or other crops. About 40 of the 100 labeled pixels were used to train clustering and maximum likelihood classification algorithms. These algorithms were used to classify the pixels of each of the other 23,000 segments. The remaining 50 labelled pixels were used to adjust the percentage of pixels computer-classified as small grain to estimate the proportion of the segment area where small grains were growing. Finally, the analyst verified the results of the classification.

Yield was estimated with multiple linear regression models of historical yields and monthly averages of temperature and precipitation:

$$\text{Yield} = \text{A (yield for average weather)} + \text{B (adjustment for technology trend)} + \text{C (effects of current weather)} \quad (1)$$

Yield models were dependent on region. Yield was estimated for larger regions and agricultural zones (e.g. the US Great Plains) by multiplying crop acreage with crop yield.

The LACIE project obtained good results for large homogenous agricultural fields such as those in the former Soviet Union and in larger regions in the US. The results were not as good for smaller fields, because the resolution of the Landsat data was too low. One should be able to improve upon the results for smaller areas by using multispectral sensors with higher spatial resolution (Chapter 3). LACIE demonstrated that remote sensing technology could be used to obtain reliable estimates of crop yield over large regions and identified some key problems in

prediction of crop yield based on remote sensing technology. Consistency of estimates between years was obtained by training the satellite data with ground data.

5.3.2 Tropical deforestation and habitat fragmentation

Deforestation has occurred in temperate and tropical regions throughout history (e.g. Tucker and Richards 1983). In recent years attention has focused on tropical forests, where as much as 50 per cent of its original extent may have been lost to deforestation in the last two decades, primarily due to agricultural expansion (Myers 1991). Global estimates of tropical deforestation vary from 69,000 km^2 yr^{-1} in 1980 (FAO/UNEP 1981a, 1981b, 1981c) to 100,000 to 165,000 km^2 annually in the late 1980s. Of the more recent estimates, 50 per cent to 70 per cent have been attributed to deforestation in the Brazilian Amazon, the largest continuous tropical forest region in the world (Myers 1991).

Tropical deforestation is a component of the carbon cycle and has profound implications for biological diversity. Deforestation increases atmospheric CO_2 and other trace gases, possibly affecting climate (IPCC 1995). Conversion of forests to cropland and pasture results in a net flux of carbon to the atmosphere, because carbon contained in forests is higher than that in the agricultural areas that replace them. The lack of data on tropical deforestation limits our understanding of the carbon cycle and climate change (IPCC 1995). Furthermore, while occupying less than 7 per cent of the terrestrial surface, tropical forests are the home to half or more of all plant and animal species (Wilson *et al.* 1988). The primary adverse effect of tropical deforestation is massive extinction of species.

Deforestation affects biological diversity in three ways: destruction of habitat, isolation of fragments of formerly contiguous habitat, and edge effects within a boundary zone between forest and deforested areas (see also Chapter 7). This boundary zone extends some distance into the remaining forest. In this zone there is greater exposure to winds; dramatic micrometeorological differences occur over short distances; easier access is possible by livestock, other non-forest animals, and hunters; and a range of other biological and physical effects occurs. The cumulative results are loss of plant and animal species in the affected edge areas (Harris 1984).

There is a wide range in current estimates of the area deforested and the rate of deforestation in Amazonia. Brazilian scientists at the Instituto Nacional de Pesquisas Espaciais (INPE) have estimated Amazonian deforestation. These unpublished studies report a total deforested area of 280,000 km^2 as of 1988, and that the average annual rate from 1978 to 1988 was 21,000 km^2 yr^{-1}. More recently, INPE (1992) has reported deforestation rates for Brazil to range from 12,000 to 25,000 km^2 yr^{-1}. Other studies have reported rates ranging from 50,000 km^2 yr^{-1} to 80,000 km^2 yr^{-1} (Skole and Tucker 1993). Additional deforestation estimates have been made for geographically limited study areas in the southern Amazon Basin of Brazil using Landsat or meteorological data. This wide range of estimates clearly indicates a need for the timely availability of reliable, spatially contiguous data sets to monitor the rate of tropical deforestation. The Landsat data record that is available since the 1970s helps to fulfill this requirement.

5.4 AVHRR BASED REGIONAL AND GLOBAL STUDIES

AVHRR data are used for very diverse purposes. This section provides an overview of sources of interference in AVHRR data and a discussion on ways to detect and correct these. Several examples of applications are presented that are based on the ability to detect interannual variation in vegetation with AVHRR NDVI data, including one example that discusses the detection of wild fires with AVHRR thermal channels. If one would like to infer vegetation seasonality from NDVI data, very few corrections are needed since the seasonality is large (in temperate forests, typically ranging from 0.1 to 0.7). On the other hand, trends in NDVI data are small, in general much less than 0.05 NDVI over a period of 10 years, and are of the same order of magnitude as errors in carefully corrected data (Malmström *et al.* 1997). Between these two extremes is the detection of interannual variation with periods of 2 to 4 years. The change in NDVI is about 0.1; hence interannual variation can be determined from carefully corrected data.

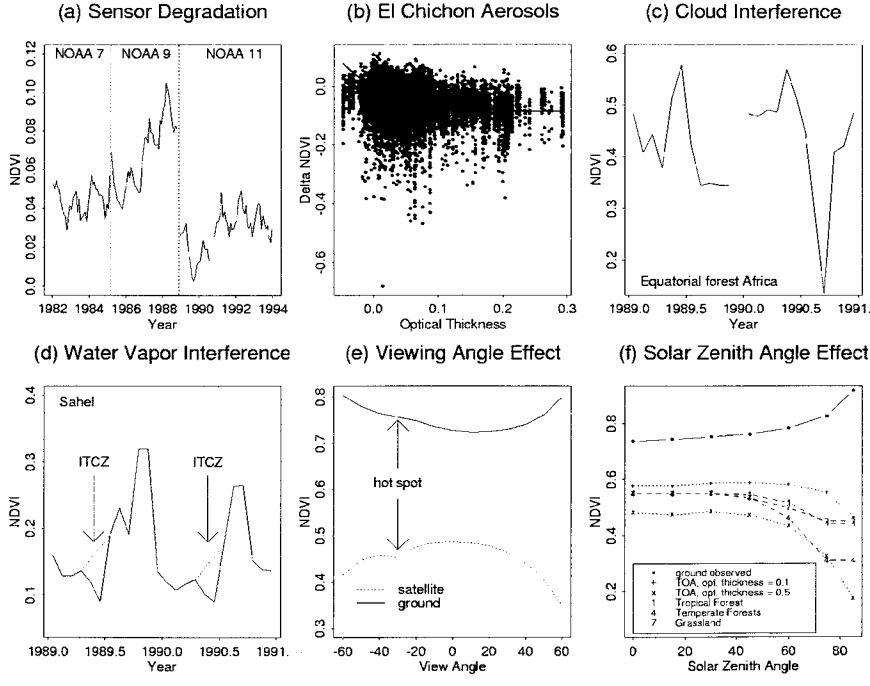

Figure 5.1. Interferences in NDVI data.

5.4.1 Sources of interference

A summary of interferences in AVHRR NDVI data is provided in Figure 5.1. Interferences are related to the sensor, the platform orbit, the atmosphere, and the land surface properties. These corrections are described in detail in Los *et al.*

(2000). Briefly Figure 5.1 shows (a) Variations in NDVI over the Saharan desert that result from calibration differences and variations in sensitivity of AVHRRs visible and near-infrared channels aboard NOAA-7, -9 and –11. (b) Decrease in NDVI with optical thickness; increased optical thickness is caused by aerosols from the El Chichon eruption. (c) Clouds result in lower or missing values over a tropical forest. (d) Decreased NDVI as a result of increased atmospheric water vapour at the beginning of the growing season in the Sahel. (e) Increase in NDVI with viewing angle for ground measurements (top line) and decrease in NDVI with viewing angle for top-of-the-atmosphere measurements. (f) Increase in NDVI with solar zenith angle for ground measurements (top line); decrease in NDVI with solar zenith angle for top-of-the -atmosphere measurements; + and x indicates different aerosol loading, 1 indicates relationship estimated from statistical analysis (from Los *et al.* 2000).

5.4.1.1 Sensor degradation

The sensitivity of the sensor changes over the time of operation of the NOAA satellite. As a result we see variations in NDVI time-series from areas such as deserts that we would otherwise expect to be invariant. Several approaches exist to correct for sensor degradation. All of these assume specific invariant targets and attribute changes in NDVI from these targets to sensor degradation; amongst these invariant targets are deserts (Rao and Chen 1994; Los 1998b), cloud tops (Vermote and Kaufman 1995), or maximum and minimum statistics collected for the entire globe (Brest *et al.* 1997). Calibration is performed in two steps; first the so-called pre-flight calibration is applied; this is the calibration that is done prior to launch. A calibration offset can also be estimated from measurements that the AVHRR takes from outer space. This so-called deep space count provides a more reliable indication of the offset than the preflight calibration offset.

A relative calibration can be obtained by selecting an arbitrary data point of a time series as a reference; absolute calibration can be obtained by using additional information, e.g., from aircraft, to adjust any point of the time series, and then adjust other points accordingly.

A slight complication is that in general deserts do exhibit some seasonality. This seasonality is most likely caused by variations in water vapour content; channel 2 is sensitive to variation in water vapour. By subtracting the seasonal cycle from the estimated r1/r2, this effect can be significantly reduced. Solar zenith angles do not significantly affect the top-of-the-atmosphere NDVI over the Sahara desert (Los 1998b).

5.4.1.2 *Atmospheric effects and correction (Figure 5.1.b and d)*

The atmosphere alters the radiation reflected from the land surface by absorption and scattering. Atmospheric water vapour and ozone are strong absorbers of solar radiation, whereas molecules and aerosols predominantly scatter (Chapter 3).

Scattering by molecules and absorption by ozone can be accounted for by using topographic data (molecular scattering) or an ozone climatology or observations from satellite (ozone). The effects of aerosols and water vapour are more difficult to account for, since their concentrations are highly variable in space and time. Aerosols increase scattering by the atmosphere in both the visible and near infrared bands. The effect of aerosols is strongest over dark dense vegetation; for these conditions the visible reflectance increases relative to the near infrared reflectance and this causes a decrease in the NDVI.

Aerosols can originate from deserts or bare soils, these aerosols remain for the most part in the troposphere, or they can originate from volcanic eruptions; part of the volcanic aerosols can reach the stratosphere. Data on tropospheric aerosols are hard to obtain and it is therefore difficult to correct for these.

Stratospheric aerosols from volcanic eruptions can remain airborne for several years. The effects of the eruptions by El Chichon (Mexico) in April 1982 and of Mt Pinatubo (the Philippines) in 1991 lingered for several years. Initially the distribution of aerosols is highly concentrated. Several months after an eruption, stratospheric aerosols are well mixed, and their concentration depends mostly on latitude and time since the eruption. The effect of aerosols can be estimated from observations over dark targets such as open water (oceans) or dark dense vegetation. Figure 5.2.b shows a plot of optical thickness values that were measured after the eruption of El Chichon in 1982 in Mexico from AVHRR data over the Pacific Ocean (Vermote *et al.* 1997) versus deviations in NDVI from areas with a mean monthly NDVI > 0.5. This relationship was used to correct the FASIR NDVI data for the effects of volcanic aerosols (Los *et al.* 2000). The aerosols affect the NDVI in a near-linear way, with the largest effects on high NDVI values from dense vegetation and negligible effects on low NDVI values from bare soils. A simple approximation of this relationship is

$$\Delta NDVI = \Delta NDVI_{max}(NDVI\text{-}NDVI_{min})/(NDVI_{max}\text{-}\Delta NDVI_{max}\text{-}NDVI_{min}) \quad (2)$$

where $\Delta NDVI$ is the expected change in NDVI as a result of volcanic aerosols; $\Delta NDVI_{max}$ is the maximum change in NDVI as a function of latitude and time; NDVI is the measured contaminated NDVI; $\Delta NDVI_{max}$ is the maximum NDVI for a particular latitude; and $NDVI_{min}$ is the minimum NDVI (minimum NDVI value over deserts). Estimates of these values are data set dependent.

5.4.1.3 *Clouds*

Clouds obscure the land surface and are especially a problem over areas with frequent rainfall and associated dense vegetation (Figure 5.1.c). Clouds have low NDVI values. The maximum value compositing, i.e. selecting the maximum NDVI over a period of 10 days, 15 days or a month, reduces the effects of clouds by selecting data from clear, cloud-free days with high NDVI values. In extreme cases,

e.g. over tropical forests, very few cloud-free data may be available. In these cases the compositing period could be expanded (e.g. to two months), or spatial filters could be used that select the maximum NDVI over a moving window of 3x3 or 5x5 pixels. The spatial or temporal resolution decreases, but a more representative value is likely selected.

Short-term variations in NDVI data that result from atmospheric aerosols or clouds can be corrected by using information from the entire time-series. One way to reduce the effect of these outliers is by fitting Fourier series through the data with linear regression. By using a weighted least squares solution, spurious data points are identified and replaced with estimates from the fitted Fourier series (Sellers *et al.* 1996b).

5.4.1.4 Solar zenith angle effects

The NDVI varies with the solar zenith angle, i.e., the angle that the sun makes with a line normal to the Earth's surface. The variation depends on the type of land surface and the atmosphere. The NDVI of dark dense vegetation tends to increase with increasing solar zenith angle when measured at the ground. At the top of the atmosphere, larger solar zenith angles lead to increased scattering and the NDVI of dark dense vegetation tend to decrease with solar zenith angle (Figure 5.1.f). Hence the effects of atmosphere and land surface in part compensate each other. The effect of the atmosphere is in general stronger, hence NDVI of dark dense vegetation measured at the top of the atmosphere tends to decrease with solar zenith angle. Solar zenith angle effects in the NDVI of bare soils tend to be small, if not negligible. The direction of solar zenith angle effect of NDVIs from sparse vegetation measured at the top of the atmosphere varies dependent on land surface properties and composition of the atmosphere. Sellers *et al.* (1996b) assume the effect to be linear with NDVI, which seems valid for some sparsely vegetated areas, but not for others.

The solar zenith angle depends on latitude, time of year and time of day. The effect of solar zenith angle on NDVI data can be estimated from a statistical analysis of NDVI distributions. First the land surface is stratified into classes with equal solar zenith angle interval and vegetation type – only vegetation types that can develop fully green conditions should be selected. NDVI histograms are calculated for each of these classes. The maxima of these histograms represent fully green conditions. The solar zenith angle effect can than be established by plotting per vegetation class, the 98 or 95 per cent of the NDVI versus the solar zenith angle interval. The green conditions represented by the 98 per cent values show a decrease in the NDVI with increased solar zenith angle (Figure 5.1). An equation for top-of-the-atmosphere solar zenith angle effect valid between solar zenith angle of 30° to 60° is given by

$$NDVI_{98} = NDVI_{98,0} - k_1(\theta - \pi/6)\text{^}k_2 \qquad (3)$$

Where $NDVI_{98,0}$ is the NDVI for an overhead sun, θ is the solar zenith angle, and k_1 and k_2 are constants that can be determined with non-linear regression. Equation 3 can also be log transformed and the constants can than be estimated with linear regression. For low vegetation conditions the analysis can be repeated for NDVI

values from bare soils using the 2 percentiles instead of the 98 percentiles. Effects of solar zenith angle on the NDVI of bare soils are in general small. After establishing the effects for minimum and maximum NDVI conditions, the data can be corrected assuming a linear effect of solar zenith angle on intermediate NDVI values

$$NDVI_0 = (NDVI_\theta - NDVI_2)(NDVI_{98,0} - NDVI_2)/(NDVI_{98,\theta} - NDVI_2) + NDVI_2 \quad (4)$$

Gutman (1999) also proposed a correction of NDVI data based on variations in low and high NDVI values, but derived land cover classes from the seasonality of NDVI time-series.

5.4.1.5 Soil background variations

Variations in reflective properties of the bare soil can result in variations in NDVI that are not related to variations in vegetation. In addition, evidence has been found that variations in atmospheric composition, e.g. water vapur, result in temporal variations in NDVI from bare soils (Rao and Chen 1994). These effects are of importance for studies in desert margins. We will find two examples that deal with soil background effects on NDVI (sections 5.4.2 and 5.4.3).

5.4.1.6 Discussion

The corrections for sensor degradation, solar zenith angle effects and volcanic aerosols are the most important ones for the study of interannual variation and are essential in many cases to do meaningful comparisons between years. Other corrections may be applied as well; corrections for ozone absorption and Rayleigh scattering will bring NDVI values closer to ground measurements. However, these corrections may come at a cost when daily data are composited; maximum value compositing on atmospherically corrected data tends to select data from off nadir-viewing angles because these are higher; maximum value compositing on uncorrected data tends to select data from near-nadir viewing angles (compare top and bottom lines in Figure 5.2.e). To avoid problems that are associated with selection of data from off-nadir viewing angles (such as a larger pixel size, overestimation of vegetation greenness, and large differences in observed vegetation greenness for slight variations in viewing angle) a BRDF correction is needed prior to maximum value compositing. The range of solar zenith angles and viewing angles from which AVHRR data are selected over a compositing period is in many cases insufficient to do a proper BRDF correction.

In the next couple of sections several AVHRR NDVI based applications are discussed.

5.4.2 Desert margin studies

The term desertification is most often used to describe the advance of desert-like conditions (UNCOD 1977). Poor land management coupled with increased

population are often blamed for catastrophic desertification in semi-arid regions such as sub-Saharan Africa. In the mid-seventies several authors reported an expansion of the Saharan desert estimated at a rate of 5.5 km per year (Lamprey 1975). This desert encroachment had direct consequences for humans, animals and plants, and could trigger a positive feedback loop on the (local) climate that would further increase the desert expansion (Charney *et al.* 1977). This positive was by an initial decrease in vegetation. Because vegetation is in general darker than the underlying soil, the total albedo of the surface and less solar radiation is absorbed by the land surface. The total energy emitted by the land surface in the form of latent and sensible heat to the atmosphere is reduced, and this reduces evapotranspiration and convection. Rainfall is reduced as a result of lower concentrations of moisture in the atmosphere and less moisture is available for plant growth. The initial reduction in vegetation thus causes a further decrease in the vegetation amount, or at least sustains itself. A similar argument can be made for the reversed mode of the feedback loop, i.e. more vegetation leads to lower albedo, more heat absorption by the land surface, higher evaporation, higher rainfall amounts and more vegetation. A positive feedback loop is by its very nature highly unstable and it is therefore obvious that the positive feedback loop between climate and vegetation is not the only mechanism at work in the Sahel. Large weather systems such as the seasonal movements of the Inter Tropical Convergence Zone (ITCZ) that are driven by warming and cooling of the oceans dominate the Sahelian rainfall. Nevertheless, the mechanism is likely to enhance variations in the local climate near desert margins however, and for this reason, expansions and contraction of desert margins are thought to be an important indicator of global climate change.

Helldén and co-workers (Helldén 1984, 1988; Olsson 1985) questioned the rate of desertification of 5.5 km per year estimated by Lamprey (1975). They showed that the high rates of desertification were derived from local areas and were not valid for the entire Sahel. Moreover, the climate in the Sahel is characterized by cycles of increasing and decreasing wet and dry conditions (Nicholson *et al.* 1988). The study of Lamprey (1975) compared data from a wet and a drought cycle and thus overestimated the rate of desert encroachment. Tucker *et al.* (1991) studied the interannual variation of AVHRR based NDVI data to investigate the rate of desertification for the entire Sahel.

The study of Tucker *et al.* (1991) used monthly GIMMS NDVI composites for Africa. The data were corrected for sensor degradation and soil background effects to determine more accurately the interannual variations in NDVI. The NDVI was corrected for sensor degradation correction by adding monthly offsets, ΔNDVI

$$NDVI_d = NDVIp + \Delta NDVI, \qquad (5)$$

where $NDVI_d$ and $NDVI_p$ stand for preflight and desert calibrated NDVI respectively. Equation 5 is an adequate approximation for sensor degradation between NDVI values of 0 and 0.3 (Los 1993). Solar zenith angle effects and volcanic aerosol effects are likely to be small because NDVI values are low. The soil background effect was estimated from areas with a standard deviation over the growing season smaller than 0.04 NDVI. For these areas NDVI values

corresponding to the highest channel 5 brightness temperatures during the end of the dry period (1 to 21 March) of 1989 were subtracted from the annual time-series. NDVI data were then summed over the growing season and a positive relationship was derived between growing season mean NDVI and annual rainfall using linear regression. By defining the Sahelian zone as the region with an average annual precipitation between 200 and 400 mm and relating this number to a seasonally summed NDVI, it became possible to detect year-on-year changes in the aerial extent of vegetation in the Sahel. These variations showed an expansion of desert like conditions in the Sahel from 1981 to 1984, which was a year of severe drought. After 1984, conditions improved which resulted in a gradual increase in the amount of vegetation in the Sahel. Superposed on this long-term trend are interannual variations in vegetation extent caused by a interannual variations in rainfall. Ellis and Swift (1988) reported that these areas are in non-equilibrium by nature, i.e. they are perturbed by abiotic forces, usually droughts.

The results from the study by Tucker clearly demonstrate that in order to assess desertification in the Sahel, data must be interpreted in relation to long-term climatic cycles of drought and wetness. It is then possible to estimate the effects of localized degradation and erosion as deviations from a long-term trend. Several authors (Helldén 1988; Olsson 1985; Prince 1991) concluded that increased rangeland activity and intensified agricultural practices led to, e.g. a shift in vegetation composition towards species not favoured by cattle, shorter periods between fallow and cultivated cycles, increased erosion, and decreased infiltration capacity of the soil. They did not find evidence for a rapid expansion of the Saharan desert.

5.4.3 Monitoring Desert Locust habitats

The Desert Locust, *Schistocerca gregaria*, is still a common threat to the vulnerable pastures, subsistence farming and agriculture in the arid and semi-arid areas of Northern and Sahelian Africa, the Middle East and southwest Asia. The control of the Desert Locust is an important part of the general effort in ensuring food security in these regions. The Food and Agriculture Organization of the United Nations (FAO) adopted a preventive control approach aimed at reducing cost, scale and environmental hazards. Early warning is the cornerstone of this preventive strategy. Locust situation evaluation and forecasting at national and global scale is a prime activity of the early warning. To be successful, timely and reliable information on various locust population and environmental parameters, such as rain and vegetation, is required.

Traditionally, Plant Protection Services organize field surveys to estimate the condition of the locust habitats, in terms of soil moisture and vegetation, and the situation of locust populations. However, field surveys are expensive, cover only small areas and cannot be frequent. Low resolution satellite remote sensing offers a more cost-effective means to obtain a synoptic overview on the ecological conditions of the natural habitat of the Desert Locust. This information helps to forewarn of suitable breeding conditions, target field surveys and thus improves their efficiency.

Rainfall is a first indicator of a potential favourable condition of the locust habitat. But there are hardly any representative weather stations and estimates from satellites are still not adequate. Vegetation development that follows rain is required by locusts for food and shelter and can be observed by satellite. In terms of cost, time frequency and area coverage, NOAA AVHRR data are very suitable for this routine monitoring task. Real time data are required. Historic data are of limited value as the rain events, triggering the vegetation growth, are too erratic in time and space in this desert environment to make historic comparison sensible. Furthermore, vegetated locust-breeding areas are rather small, mostly not more than a few square kilometers. When applying NOAA GAC (4 km) data, it was experienced that many of these vegetated patches, important though for locust breeding, were not detected at this coarse resolution. The 1 km pixel size of the NOAA LAC/HRPT data proved to be more adequate.

Projects at FAO want to make the NOAA AVHRR vegetation index (NDVI) (Tucker *et al.* 1984 and 1986b) products more applicable to the non-technical locust control staff. This includes the development of methods to increase the reliability of the NDVI as well as providing the tools for integrating the NOAA NDVI with other spatial information, such as maps on soil conditions, potential vegetation or locust suitability, to improve the final interpretation.

In relation to monitoring locust-breeding areas from an early warning perspective, Hielkema *et al.* (1986) proposed an analytic approach by synthesizing, based on a geographical grid, single NDVI values, above a certain threshold, into a factor that would represent potential suitable conditions for breeding. This approach took into consideration the restricted computing power on the user's side at that time. Application of the method quickly shed light on one of the basic shortcomings of the NOAA NDVI. The unpredictable variation in space and time of NDVI values imposing the inability of defining reliable thresholds to distinguish soil from vegetation consistently over one image and throughout a season.

The reliability of the NDVI applied for locust habitat monitoring is hampered by a weak reflectance of the low plant cover, typical for the desert breeding areas. This enhances the problem of soil reflectance interference on the NDVI. Variations in soil reflectance and spectral characteristics of quartzite desert soils, affect the vegetation index. Improvement of the NOAA NDVI, to represent truly the vegetation cover on the ground, can be obtained by standardizing the background reflection (Cherlet and Di Gregorio 1993). An insight this work provoked was the consideration that by applying similar procedures the NDVI can be somehow improved, strongly depending on the geo-physical aspects of the area, but that limits are now reached in terms of NOAA sensor and data quality and sensitivity for desert vegetation monitoring. Improvements can be expected when satellite sensors with spectral bands more adapted to vegetation detection and better geometric correction of images become available at the same 1 km resolution. However, high spatial resolution imagery indicated that further improvements would be reached with higher resolutions than 1 km, such as 500 m or even 250 m. Similar time frequency, area coverage and cost of data would be required, though, to keep the same advantages with regard to cost-efficient monitoring.

Apart from these tentative improvements to the NOAA NDVI data itself, the routine and operational interpretation of the NDVI for desert habitat monitoring is made more reliable by integrating the data in a GIS application. An integrated

information system, RAMSES (Reconnaissance And Management System for the Environment of *Schistocerca* i.e. Desert Locust), was developed to support the national locust early warning efforts. A custom-made user interface makes it easy for the non-specialists to access a variety of data, such as locust information, rainfall, locust habitat data and remote sensing products, such as the NDVI. The land unit map contains a linked database inventorying the important environmental parameters. This spatial information is an aid to a more correct interpretation of the NOAA NDVI in view of evaluation of locust habitat conditions.

The main impact of using routinely NOAA AVHRR NDVI products integrated with field data on locust and their habitat and meteorological data is a significant contribution to decision-making procedures for Desert Locust survey and control planning. Timing of surveys can be optimally planned. Surveys can be reduced to cover habitats estimated to be suitable for breeding. Early detected potential hazard areas can be monitored, increasing the preparedness for intervention. Subsequent control operations become sharply targeted. This can save time, available resources and reduces hazardous environmental impact of chemical campaign control efforts.

5.4.4 Land cover classification

The use of satellite data for the classification of land cover types is a useful addition to classical methods that use observations from ground surveys. In general, satellite based land cover classifications have used Landsat and SPOT imagery. Most authors claim classification accuracies of between 60 per cent and 90 per cent, dependent on the scale of the object being mapped (for example, using the Anderson scale, are you mapping forest from soil, coniferous forest from deciduous forest, or specific forest types such as oak or aspen), availability of training data and separability of classes (Skidmore *et al.* 1988). Land surface classifications from a combination of satellite and ground data can be obtained at a lower cost when compared to classifications solely based on ground surveys and aerial photograph interpretation. Landsat and SPOT based land cover classifications generally cover areas the size of one or a few scenes, the size of one Landsat scene being about 185 by 185 km.

Land cover classifications for areas the size of continents or for the entire globe are used for different purposes than the classifications from Landsat or SPOT scenes and generally require less detail both in the distinction of the number of classes and the spatial resolution of the data. These classifications, based on NOAA AVHRR images, are used to provide input parameters to mesoscale and global scale climate and carbon models (Dorman and Sellers 1989; Henderson Sellers and Pitman 1992; Field *et al.* 1995). Examples are the classifications by Matthews (1983), Kuchler (1983), and Wilson and Henderson-Sellers (1985) derived for climate models and by Olson *et al.* (1983) derived for carbon models (see also Chapter 6). These global classifications are compiled from ground based sources such as atlases, local maps, and reports. The output from these classifications often have large inconsistencies and errors because of differences in class definitions and interpretation, inclusion of outdated material, differences in spatial detail and scale, and the purpose for which the material was derived.

For example, Tucker *et al.* (1985a) made a land cover classification of Africa based on the first two principal components of three week composites of the NOAA-GVI data set over a 19 month period (April 1982 until November 1983). The first principal component was related to the average NDVI over the year, and the second principal component was related to the magnitude of the annual cycle. The results of the classification show a qualitative agreement with the major vegetation types found by White (1983), although deviations were found in several areas. Tucker *et al.* (1985a) suggested refinements of the method and additional years of data to improve the classification.

DeFries and Townshend (1994) provide a systematic discussion of limitations to land cover classifications based on NDVI time-series. They found that temporal profiles may not always be distinguishable, e.g., similar land cover types may have different temporal profiles and different land cover types may have similar profiles. Another complication is that identical land cover types may have similar temporal NDVI profiles but with a shift in the phase as a result of differences in the timing of the seasons. The reversed seasonality on the Northern and Southern Hemispheres is an example.

As a first approach to global classifications based on NDVI time-series, data are analyzed by region or by continent. This, of course, has limitations because it does not address climate gradients within a region and it limits the number of pixels for training areas and may give less reliable results. A second approach is to use additional information, for example data could be stratified by latitude and data could be classified by latitude interval. The strong latitudinal dependency of the occurrence of land cover types will lead to a small loss of training sites per class. The added information helps to distinguish between classes with otherwise similar profiles. A third approach is to standardize the timing of the temporal profiles, by shifting the profiles until the month of maximum NDVI is the same for all time-series. A fourth, in some ways related approach, is to run the classification on temporal characteristics of the NDVI time-series such as the average annual NDVI, the maximum range in NDVI values during the year, the length of growing season, and the rapidity of the rate of greening and senescence. These latter two techniques, without further information, do not solve the problems of distinguishing different vegetation classes with a similar temporal profile. To improve classifications, Loveland *et al.* (1991) used several measures of NDVI time-series (maximum NDVI, start of growing season, month with maximum NDVI and so on) in combination with climate data (mean precipitation and temperature), elevation, ecoregions and land resource data.

The identification of reliable training sites for global land cover classifications is an important issue. DeFries and Townshend (1994) used three data sets (Matthews 1983; Olson *et al.* 1983; Wilson and Henderson-Sellers 1985) and identified areas where there was agreement between these data sets. An alternative way to obtain training sites is from the interpretation of SPOT and MSS imagery, and to scale the results to the size of AVHRR pixels or global 1° by 1° grid cells. The reliability of the classification can be assessed by the spectral separability of the classes from training sites, and by testing the classification on sites not used for training the classes. Sensor degradation effects, solar zenith angle effects and volcanic aerosol are of minor importance because firstly, only one year of data is analyzed at the time and secondly, the AVHRR classification is directly

trained with interpretations of Landsat data. These effects, as well as the uncertainties in the classification, do become serious issues if one would like to compare classifications from different years.

Results of NDVI based land cover classifications by Tucker *et al.* (1985a), Loveland *et al.* (1991) and DeFries and Townshend (1994) showed promise but also revealed that the accuracy is not as good as the accuracy of MSS or SPOT based classifications. However, Loveland *et al.* 1991 reported improvements in large area classifications with AVHRR data compared with large area classifications from conventional ground surveys. Further improvements should be obtained by incorporation of additional data, for example additional spectral channels, BRDF properties of the land surface, and climate data, and by use of higher spatial and spectral resolution data, such as from the MODIS instrument.

5.4.5 ENSO

Interannual variations in NDVI data are linked to interannual climate perturbations such as the El Niño Southern Oscillation (ENSO) phenomenon. The NDVI record of 18 years provides a unique basis for studying climate variability in areas where climatic data such as rainfall data are sparse.

One important aspect in understanding the response patterns of the land biosphere to interannual climate variability is in determining regions of the world that show a marked response to climate variability. The ENSO phenomenon is a principal cause of global interannual climate variability. ENSO events are triggered by the anomalous warming of oceanic waters in the central to eastern Pacific Ocean. The warming of the eastern Pacific is associated with lower than normal barometric pressure at Tahiti and higher than normal pressure over Darwin, Australia. This seesaw in sea level pressure between these two stations, termed Southern Oscillation Index (SOI) is the most commonly used index for ENSO phenomena and permits the identification of warm and cold ENSO events back to the late 19th century. Strong negative anomalies are associated with weakening easterly winds and a sea surface temperature warming of equatorial Pacific waters off the South American coast which is also referred to as an 'El Niño' event. The reverse of these conditions or cooling of oceanic waters in the eastern Pacific is termed 'La Nina'. Anomalous climatic conditions caused by ENSO such as increased rainfall or occurrence of drought is linked with outbreaks of human and livestock diseases in various countries. During the warm phase of ENSO there is a tendency for above normal rainfall in the eastern Pacific and below normal rainfall in the western Pacific Belt and eastern Indian Ocean. The climatic conditions are typically opposite during cold ENSO events or La Ninas. Over Africa there is tendency for differential hemispheric response patterns, with Eastern Africa receiving above normal rainfall and dry conditions prevailing over Southern Africa during warm ENSO events and the opposite effects during cold events. Occurrences of the warm ENSO phase have been linked to increased rainfall, increased vegetation growth and outbreaks of Rift Valley Fever in East Africa.

Principal component analysis is a powerful way to reduce data volumes and find associations between variables in the data. Principal components analysis in the time domain has been used to detect seasonal signals (Eastman and Fulk 1993;

Andres *et al.* 1994) and interannual signals in vegetation that are related to ENSO (Eastman and Fulk 1993; Anyamba and Eastman 1996).

Figure 5.2 shows a comparison between principal components loadings from a PCA analysis of a monthly NDVI time series for Africa for the period 1986 – 1990. The comparison with Sea Surface Temperature (SST) anomalies from the eastern Pacific NINO3.4 region shows an inverse relationship with NDVI variability in Southern Africa detected by the PCA. During the 1986/87 warm ENSO event, SSTs in the Pacific are warmer than normal while NDVI is below normal (negative loadings) because of below normal rainfall in southern Africa.

During the cold phase (La Nina), SSTs in the eastern Pacific are below normal and NDVI over Southern Africa is above normal. This pattern is illustrative of ENSO teleconnections, where by changes in the ocean-atmosphere coupling in the Pacific, impact rainfall and thus vegetation greenness at distant or remote locations from the Pacific (Ropelewski and Halpert 1987, 1989).

Rainfall data have incomplete spatial coverage and show gaps in temporal records. Satellite vegetation index data provide contiguous spatial coverage and complete time-series. This continuous coverage allows monitoring of the spatial and temporal development of a drought. This may provide important clues about the outbreak of tropical diseases that are related to extremes in climate (Nicholls 1991).

For example it has been shown that Rift Valley Fever (RVF) outbreaks in East Africa are associated with periods of negative SOI (El Niño) periods associated with heavy rainfall (Figure 5.3).

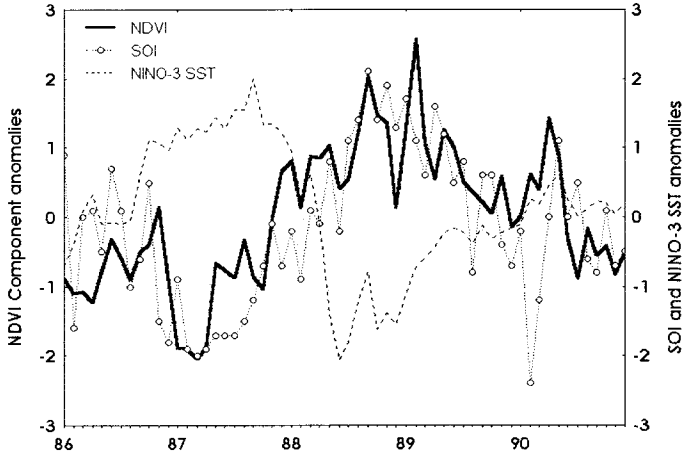

Figure 5.2: Comparison between NDVI component anomalies for Southern Africa against NINO3.4 SST and SOI anomalies for the period 1986–1990.

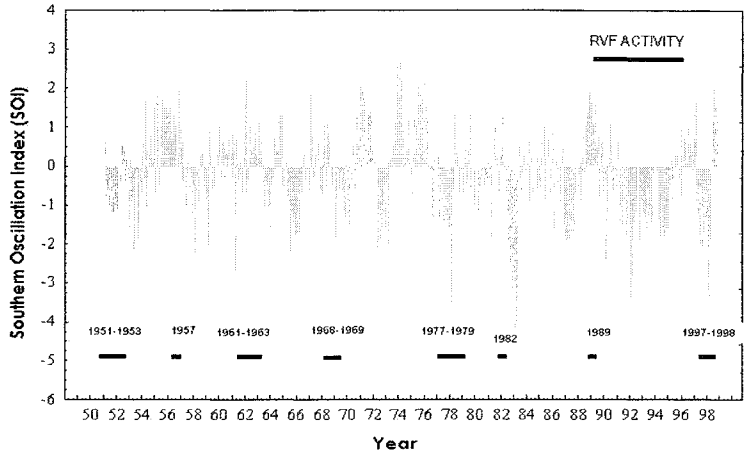

Figure 5.3: RVF outbreak events superimposed upon the Southen Oscillation Index (SOI) for the period 1950–1998. Outbreaks have a tendency to occur during the negative phase of SOI which is associated with above normal rainfall over East Africa.

Such heavy rainfall floods mosquito breeding habitats in East Africa, known as *dambos*, that are good habitats for *Culex* species mosquito vectors that transmit RVF. Areas that are experiencing anomalous climatic conditions, in this case increased rainfall and associated vegetation greenness, can be identified with NDVI time series (Linthicum *et al.* 1999).

5.5 WILD FIRE DETECTION

The detection of high-temperature sources using the AVHRR was first proposed by Dozier in 1981 (Dozier 1981; Matson and Dozier 1981). Since that time, the greater appreciation of biomass burning as a major factor in the emission of trace gases, and the resulting effect upon climate change, has led to an extensive body of research concerning satellite-based fire detection (Langaas 1995).

A typical land surface, which is approximately a 300 K black body, emits far more energy at 10.8 μm than at 3.8 μm. At typical smoldering and flaming temperatures of 500 to 1200 K, however, the emitted energy at 3.8 μm greatly exceeds that emitted at 10.8 μm. A subpixel high temperature source, such as a fire, will consequently elevate the observed response in NOAA AVHRR channel 3 compared to that of channel 4. This characteristic difference in response is exploited when looking for active fires.

In practice, AVHRR-based fire detection is complicated by the fact that other phenomena unrelated to burning produce the same characteristic signature. The most significant of these is reflected sunlight, which has a substantial 3.8 μm component. The relatively low saturation levels of the thermal bands (for land) further complicate AVHRR-based fire detection.

Most of the existing operational AVHRR fire detection algorithms have been developed for regional application and have been tuned accordingly. In light of the extensive range of biomes in which biomass burning may occur, however, more recent efforts have focussed on the development of detection algorithms that may be applied globally (Giglio *et al.* 1999). Generally, the techniques utilize similar processing steps and input data, and can be placed into two broad categories: fixed-threshold techniques and contextual techniques (Justice and Dowty 1994). Fixed threshold algorithms generally rely on preset absolute thresholds and consider a single pixel at a time, while contextual methods compute relative thresholds based upon statistics calculated from neighboring pixels.

As the majority of remotely sensed fire fronts are less than 1 km^2 in size, most AVHRR fire detection algorithms use 1 km LAC or HRPT data. In some instances GAC observations have been found to be useful (Koffi *et al.* 1996), but the severe sampling and averaging used to create the coarser resolution GAC data eliminates a significant number of fire pixels that would otherwise be detected.

5.6 DISCUSSION

Remote sensing of the global biosphere has developed from a qualitative science towards a quantitative science. During the early years satellite data were used as an observational tool to obtain information about the distribution of different types of land cover. AVHRR data allowed monitoring of the seasonality of vegetation. Comparison of AVHRR data between years created a need for corrections of the data. Newer satellite systems were designed to avoid many of the problems inherent with using AVHRR imagery. Improved calibration of data and improved corrections permit more straightforward comparisons between years.

The long-term record of Landsat and AVHRR data has provided us with unique insights in the functioning of the global biosphere and provided us a better understanding of seaonality of vegetation around the globe, rates of tropical deforestation and land cover change. We show several examples of studies that used either high spatial resolution or high temporal resolution data. In some cases a need exists for both; several applications indicated that the 4 km pixel size was a limitation (e.g. Locust breeding, fire detection). Better results are expected from higher resolution sensors with at least the same recurrence time as the AVHRR (e.g. Terra-MODIS, ENVISAT). Other applications, such as detection of an earlier growing season, do not require higher spatial resolution data, but would benefit from higher temporal resolution data. More frequent coverage would increase the probability of obtaining cloud-free data for a shorter period of time and would more accurately establish the start and end of the growing season.

5.7 REFERENCES

Andres, L., Salas, W. A., and Skole, D., 1994, Fourier analysis of multi-temporal AVHRR data applied to a land cover classification. *International Journal of Remote Sensing*, **15**, pp. 1115-1221.

Anyamba, A. and Eastman, J.R., 1996, Interannual variability of NDVI over Africa and its relation to El Nĩo Southern Oscillation, *International Journal of Remote Sensing*, **17**, 2533-2548.

Brest, C.L., Rossow, W.B. and Roitier, M.D., 1997, Update of radiance calibrations for ISCCP, J. Atmos. *Oceanic Technolo.* **14**, 1091-1109.

Charney J., Quirk, W.J. Chow, S.H. Kornfield, J., 1977, Comparative study of effects of albedo change on drought in semi-arid regions, *Journal of Atmos. Sciences*, **34**, 1366-1385.

Cherlet M.R., and Di Gregorio, A., 1993, *Calibration and Integrated Modelling of Remote Sensing Data for Desert Locust Habitat Monitoring*, FAO RSC series N. 64, 115pp.

DeFries, R.S., and Townshend, J., 1994, NDVI-derived land-cover classifications at a global scale, *International Journal of Remote Sensing*, **15**, 3567-3586.

Dorman, J. L., and Sellers, P. J., 1989, A global climatology of albedo, roughness length and stomatal resistance for atmospheric general circulation models as represented by the simple biosphere model (SiB). *Journal of Applied Meteorolgy*, **28**, 833-855.

Dozier, J., 1981, A Method for Satellite Identification of Surface Temperature Fields of Subpixel Resolution. *Remote Sensing of Environment*, **11**, 221-229.

Eastman R.J., and Fulk, M., 1993, Long sequence time-series evaluation using standardized principle components, *Photogrammetric Engineering and Remote Sensing*, **59**, 1307-1312.

Eischeid, J.K., Diaz, H.F. Bradley, R.S. and Jones, P.D., (eds), 1991, *A comprehensive precipitation dataset for global land areas.* U.S. Dept of Energy, Washington D.C., 82 pp.

Ellis, J.E. and Swift, D.M., 1988, Stability of African pastoral ecosystems: Alternate paradigms and implications for development. *Journal of Range Management*, **41**, 450-459.

FAO/UNEP, 1981a, *Los Recursos Forestales de la America Tropical*, 32/6.1301-78-04, Technical Report No. 1. Rome, Food and Agriculture Organization of the United Nations.

FAO/UNEP, 1981b, *Forest Resources of Tropical Africa*, 32/6.1301-78-04, Technical Report No. 2. Rome, Food and Agriculture Organization of the United Nations.

FAO/UNEP, 1981c, *Forest Resources of Tropical Asia*, 32/6.1301-78-04, Technical Report No. 3. Rome, Food and Agriculture Organization of the United Nations.

Field, C.B., Randerson, J.T. and Malmstrom, C.M., 1995, Global net primary production: combining ecology and remote sensing. *Remote Sensing of Environment*, **51**, 74-88.

Fung I.Y., Tucker, C.J. and Prentice, K.C., 1987, Application of AVHRR vegetation index to study atmosphere-biosphere exchange of CO2. *Journal of Geophysics Resources*, **92**, 2999-3015.

Giglio, L., Kendall, J., and Justice, C. O., 1999, Evaluation of Global Fire Detection Algorithms Using Simulated AVHRR Infrared Data. *International Journal of Remote Sensing*, **20**, 1947-1985.

Goulden, M.L., Munger, J.W. Fan, S.M. Daube, B.C. and Wolfsy, S.C., 1996, Exchange of carbon dioxide by a deciduous forest: Response to interannual climate, *Science*, **271**, 1576-1578.

Goulden, M.L., Wofsy, S.C. Harden, J.W. Trumbore, S.E. Crill, P.M. Gower, S.T. Fries, T. Daube, B.C. Fan, S.M. Sutton, D.J. Bazzaz, A. and Munger, J.W., 1998, Sensitivity of boreal forest carbon balance to soil thaw, *Science*, **279**, 214-217.

Goward S.N., and Dye D.G., 1987, Evaluating North American net primary productivity with satellite observations, *Advanced Space Resources*, **7**, 165-174.

Gutman, G.G.. 1999, On the use of long-term global data of land reflectances and vegetation indices derived from the advanced very high resolution radiometer, *Journal of Geophysics Resources*, **104**, 6241-6255.

Gutman G.G., Ignatov, A. and Olson, S., 1994, Towards better quality of AVHRR composite images over land: reduction of cloud contamination. *Remote Sensing of Environment*, **50**, 134-148.

Hall, F.G., Huemmrich, K.F. Goetz, S.J. Sellers, P.J. and Nickeson, J.E., 1992, Satellite remote sensing of surface energy balance: Success, failures, and unresolved issues in FIFE. *Journal of Geophysics Resources*, **97**, 19061-19089.

Hall, F.G., Sellers, P.J. Apps, M. Baldocchi, D. Cihlar, J. Goodison, and B. Margolis, H., 1993, BOREAS: Boreal Ecosystem-Atmosphere Study, IEEE Geoscience Remote Sensing Society Newsletter, March, 9-17.

Harris, L.D., 1984, *The Fragmented Forest: Island Biogeographic Theory and the Preservation of Biotic Diversity*. Chicago, University of Chicago Press.

Helldén, U., 1984, Remote sensing for drought impact assessment - A study of land transformation in Kordofan, Sudan. *Advanced Space Resources*, **4**, 165-168.

Helldén, U., 1988, Desertification monitoring; is the desert encroaching? *Desertifcation Control Bulletin*, **17**, 8-12.

Henderson-Sellers, A., and Pitman, A.J., 1992, Land-surface schemes for future climate models: specification, aggregation, and heterogeneity. *J. Geophys. Res.*, **97**, 2687-2696.

Hielkema, J.U., 1990 Operational environmental satellite remote sensing for food security and locust control by FAO. The ARTEMIS and DIANA systems. In: Proceedings of the ISPRS, Session: Global Monitoring TP-1, 18 Sept 1990, Victoria, B.C., Canada.

Hielkema, J.U., J. Roffey, and C.J. Tucker, 1986, Assessment of Ecological Conditions Associated with the 1980/81 Desert Locust Plague Upsurge in West Africa Using Environmental Satellite data, *Int. J. Remote Sensing*, **7**, 1609-1622.

Holben, C.J., 1986 Characteristics of maximum-value composite images for temporal AVHRR data. *Int. J. Remote Sens.*, **7**, 1435-1445.

INPE, 1992, Deforestation in Brazilian Amazonia (Instituto Nacional de Pesquisas Espaciais, Sao Jose dos Campos, Brazil).

IPCC, Intergovernmental Panel on Climate Change, 1995, The IPCC Second Assessment Synthesis of Scientific-Technical Information Relevant to Interpreting Article 2 of the UN Framework Convention on Climate Change. Cambridge, Cambridge University Press.

James, M. E. and Kalluri, S. N. V., 1994. The Pathfinder AVHRR land data set: An improved coarse resolution data set for terrestrial monitoring. *International Journal of Remote Sensing*, **15**, 3347-3363.

Jones, P.D., *et al.*, (ed.), 1985, Grid point surface air temperature dataset for the Northern Hemisphere. U.S. Dept of Energy, Washington D.C., 251 pp.

Justice, C.O., and Dowty, P., (ed.), 1994, IGBP-DIS Satellite Fire Detection Algorithm Workshop Technical Report. IGBP-DIS Working Paper, 9, 88 pp., February 1993, NASA/GSFC, Greenbelt, Maryland.

Justice, C.O. (ed.), 1986, Monitoring the grasslands of semi-arid Africa using NOAA-AVHRR data. *Int. J. Remote Sens.*, **7**, 1383-1622.

Keeling C.D., Chin, J.F.S. and Whorf, T.P., 1996, Increased activity of northern vegetation inferred from atmospheric CO2 measurements, *Nature,* **382**, 146-149.

Kimes, D.S., Holben, B.N. Tucker, C.J. and Newcomb, W.W., 1984, Optimal Directional View Angles for Remote-Sensing Missions. *Int. J. Rem. Sens.*, **5**, 887-908.

Koffi, B., Grégoire, J.-M., and Eva, H., 1996, Satellite Monitoring of Vegetation Fires on a Multi-Annual Basis and at Continental Scale, in Africa. In: *Biomass Burning and Global Change*, Levine, J. S. (ed.), Cambridge, MA, MIT Press.

Kuchler, 1983, World map of natural vegetation. Goode's World Atlas, 16th edition. , New York, Rand McNally.

Lamprey, H. F., 1975, Report on the desert encroachment reconnaissance in northern Sudan, 21 October to 10 November 1975. UNESCO/UNEP, Nairobi. Republished in Desertification Control Bulletin, **17**, 1-7.

Langaas, S., 1995, A Critical Review of Sub-Resolution Fire Detection Techniques and Principles Using Thermal Satellite Data, Ph. D. Dissertation, Department of Geography, University of Oslo, Norway.

Linthicum K.J., Anyamba, A. and Tucker, C.J., 1999, Climate and satellite indicators to forecast Rift Valley Fever epidemics in Kenya, *Science*, **285**, 397-400.

Los, S.O., 1993, Calibration adjustment of the NOAA AVHRR normalized difference vegetation index without recourse to component channels, *Int. J. Rem. Sens.,* **14**, 1907-1917.

Los, S.O., 1998a, Linkages Between Global Vegetation and Climate: An analysis based on NOAA Advanced Very High Resolution Radiometer Data. NASA Report GSFC/CR-1998-206852, NASA-CASI, Hanover Maryland. 199 pp

Los, S.O., 1998b, Estimation of the ratio of sensor degradation between NOAA-AVHRR channels 1 and 2 from monthly NDVI composites. *IEEE Transactions on Geoscience and Remote Sensing,* **36**, 206-213.

Los, S.O., Collatz, G.J. Sellers, P.J. Malmström C.M., Pollack, N.H. DeFries, R.S. Bounoua, L..Parris, M.T Tucker, C.J. and Dazlich, D.A, 2000, A global 9-year biophysical land-surface data set from NOAA AVHRR data. *J Hydrometeor.,* **1**, 183-199..

Los, S.O., G.J. Collatz, P.J. Sellers, L. Bounoua, and C.J. Tucker, 2001, Interannual variation in global vegetation, precipitation, land-surface temperature and sea-surface temperatuet al hese areas. *J. Climate* **14**, 1535-1549.

Loveland, T.R., Merchant, J.W. Ohlen, D.O. and Brown, J.F., 1991, Development of a land cover based characteristics database for the conterminous U.S., *Photogram. Eng. Remote Sens.*, **57**, 1453-1463.

MacDonald, R.B., and Hall, F.G. 1980, Global crop forecasting, *Science*, **208**, 670-674.

Malingreau, J. P., Stevens, G., and Fellows, L., 1985, Remote sensing of forest fires: Kalimantan and North Borneo in 1982-83. *Ambio*, **14**, 314-321.

Malmström CM, Thompson, M.V., Juday, G.P., Los, S.O., Randerson, J.T. and Field, C.B., 1997, Interannual variation in global-scale net primary production: Testing model estimates. *Global Biogeochemical Cycles*, **11**, 367-392.

Mann, M.E., and Park, J., 1996, Joint spatio-temporal modes of surface temperature and sea level pressure variability in the northern hemisphere during the last century, *J. Climate*, **9**, 2173-2162.

Matson, M., and Dozier, J., 1981, Identification of sub resolution High Temperature Sources Using a Thermal IR Sensor. *Photogrammetric Engineering and Remote Sensing*, **47**, 1311 - 1318.

Matthews, E., 1983, Global Vegetation and Land Use: New High-Resolution Data Bases for Climate Studies. *J. Climate App. Meteor.*, **22**, 474-487.

Menzel A, and Fabian, P., 1999, Growing season extended in Europe, *Nature*, **397**, 659-659

Monteith, J. L. and Unsworth, M. H., 1990, Principles of Environmental Physics, 2nd edition, London, Edward Arnold.

Myers, N., 1991, Tropical forests - Present status and future outlook, *Climatic Change,* **19**, 3-32.

Myneni, R.B., Keeling, C.D., Tucker, C.J., Asrar, G., and Nemani R.R., 1997, Increased plant growth in the northern high latitudes from 1981 to 1991, *Nature*, **386**, 698-702.

Myneni R.B., Los S.O., Tucker C.J., 1995, Satellite-based identification of linked vegetation index and sea surface temperature anomaly areas from 1982-1990 for Africa, Australia and South America, *Geophys Res. Let.*, **23**, 729-732.

Nicholls, N., 1991, Teleconnections and health. In: M.H. Glantz, Katz, R.W. and Nicholls, N. (ed.), pp. 493-510, New York, Cambridge University Press.

Nicholson, S. E., Kim, J. and Hoopingarner, J., 1988, Atlas of African Rainfall and its Interannual Variability. Talahassee, Florida, Department of Meteorology, Florida State University.

Olson, J.S., Watts J. and Allison, L., 1983, Carbon in live vegetation of major world ecosystems. Report No. W-7405-ENG-26, U.S. Dept. of Energy, Oak Ridge National Laboratory.

Olsson, L., 1985, Desertification or climate? Investigation regarding the relationship between land degradation and climate in the central Sudan. PhD Thesis. Lunds Studies in Geography XCVIII, Department of Geography, University of Lund, Lund, Sweden.

Potter, C.S., Randerson, J.T. and Field, C.B., 1993, Terrestrial ecosystem production: a process model based on global satellite data. *Global Biogeochem. Cycles*, **7**, 811-841.

Prince, S. D., 1991, Satellite remote sensing of primary production: comparison of results for Sahelian grasslands. *Int. J. Remote Sens.*, **12**, 1301-1311.

Prince, S.D., and Justice, C.O. (ed.), 1991, Coarse resolution remote sensing of the Sahelian environment. *Int. J. Remote Sens.*, **12**, 113-1421

Prince, S.D., Kerr, Y.H., Goutorbe, J.–P., Lebel, T., Tinga, A., Bessemoulin, P., Brouwer, J., Dolman, A.J., Engman, E.T., Gash, J.H.C., Hoepffner, M., Kabat, P., Monteny, B.F., Said, F., Sellers, P., and Wallace, J. 1995, The Hydrologic Atmospheric Pilot Experiment in the Sahel (HAPEX–Sahel). *Remote Sensing of Environment*. **51**, 215–234.

Qi, J., Chehbouni, A. Huete, A.R. Kerr, Y.H. and Sorooshian, S., 1994, A modified soil adjusted vegetation index. *Remote Sens. Environ.*, **48**, 119-126.

Randerson, J.T., Field, C.B., Fung, I., and Tans, P., 1999, Increases in early season ecosystem uptake explain changes in the seasonal cycle of atmospheric CO2 at high northern latitudes. *Geophys. Res. Let.*, **26**, 2765.

Rao, C.R. and Chen, J., 1994, Post-launch calibration of the visible and infrared channels of the advanced very high resolution radiometer on NOAA-7, -9, and 11 spacecraft. NOAA Technical Report NESDIS-78, National Oceanic and Atmospheric Administration, Washington DC 20233, 1994.

Reynolds, R.W., and Marsico, D.C., 1993, An improved real-time global sea-surface temperature analysis, *J. Climate*, **6**, 114-119.

Ropelewski, C.F., and Halpert , M.S., 1987, Global and regional scale precipitation patterns associated with the El Niño - Southern Oscillation, *Monthly Weather Rev*, **115**, 1606-1626.

Ropelewski, C.F., and Halpert, M.S., 1989, Precipitation patterns associated with the high index phase of the Southern Oscillation. *Journal of Climate*, **2**, 268-283.

Rosborough, G.W., Baldwin, D.G. , and Emery, W.J., 1994, Precise AVHRR image navigation, *IEEE Trans. Geosci. Remote Sens.*, **32**, 654-657.

Roujean, J.L., Leroy, M. Deschamps, P.Y., 1992, A bidirectional reflectance model of the earth's surface for the correction of remote sensing data, *J. Geophys. Res.-Atmos.*, **18**, 20455-20468.

Sellers, P.J., and Hall, F.G., 1992, FIFE in 1992: Results, scientific gains, and future research directions. *J. Geophys. Res.*, **97**, 19,091-19,109.

Sellers, P.J., Bounoua, L., Collatz, G.J., Randall, D.A., Dazlich, D.A., Los, S. O., Berry, J.A., Fung, I., Tucker, C.J., Field, C.B. and Jensen, T.G, 1996a, Comparison of radiative and physiological effects of doubled atmospheric CO_2 on climate. *Science*, **271**, 1402-1406.

Sellers, P.J., Los, S.O., Tucker C. J., Justice C.O., Dazlich, D.A., Collatz, G.J. and Randall, D.A., 1996b, A revised landsurface parameterization (SiB2) for GCMs. Part 2: The generation of global fields of terrestrial biophysical parameters from satellite data, *J. Climate*, **9**, 706-737.

Sellers, P.J., Randall, D.A., Collatz, G.J., Berry, J.A., Field, C.B., Dazlich D.A., Zhang, C. and Bounoua, L., 1996c, A revised land-surface parameterization (SiB2) for GCMs. Part 1: Model Formulation. *J. Climate*, **9**, 676-705.

Skidmore, A.K., 1988. Predicting bushfire activity in Australia from El Niño/Southern Oscillation events. *Australian Forestry,* **50**, 231-235.

Skidmore, A.K., Bijker, W., Schmidt, K., Kumar, L., 1998, Use of Remote Sensing and GIS For Sustainable Land Management. *ITC Journal* **1997(3/4)**,302-315.

Skole D. and Tucker, C.J., 1993, Tropical deforestation and habitat fragmentation in the Amazon - Satellite data from 1978 to 1988, *Science*, **260**, 1905-1910.

Stowe, L.L., McClain, E.P., Carey, R.M., Pellegrino, P.P., Gutman, G.G., Davis, P., Long, C. and Hart, S., 1991, Global distribution of cloud cover derived from NOAA/AVHRR operational satellite data. *Adv. Space Res.*, **3**, 51-54.

Tanre D., Holben, B.N. and Kaufman, Y.J., 1992, atmospheric correction algorithms for NOAA-AVHRR products: Theory and application. *IEEE Trans. Geosci. Remote Sens.*, **30**, 231-248

Tans, P.P., Fung, I.Y. Takahashi, T., 1990, Observational contraints on the global atmospheric CO_2 budget, *Science*, **247**, 1431-1438.

Tarpley, J.D., Schneider, S.R., and Money, R.L., 1984, Global vegetation indices from the NOAA-7 meteorological satellite. *J. Climate Applied Meteor.*, **23**, 491-494.

Tucker, C. J., 1979, Red and photographic infrared linear combinations monitoring vegetation. *Remote Sens. Environ.*, **8**, 127-150.

Tucker, C.J., 1996, History of the use of AVHRR data for land applications. In: Advances in the Use of NOAA AVHRR Data for Land Applications. In: G. D'Souza *et al.* (ed.). ECSC, EEC, EAEC, Brussels and Luxembourg, pp. 1-19.

Tucker R.P. and J.F. Richards, 1983, Global Deforestation and the Nineteenth Century World Economy. , Durham, NC, Duke University Press.

Tucker, C.J., Holben, B.N. Elgin, J.H. and McMurtrey, J.E., 1981, Remote sensing of total dry matter accumulation in winter wheat. *Remote Sens. Environ.*, **11**, 171-189.

Tucker, C.J., VanPraet, C.L., Boerwinkel, E. and Gaston, A., 1983, Satellite remote sensing of total dry accumulation in the Senegalese Sahel. *Remote Sens. Environ.*, **13**, 461-474.

Tucker, C.J., Gatlin, A. and Schneider, S.R., 1984, Monitoring vegetation in the Nile Delta with NOAA-6 and NOAA-7 AVHRR. *Photogrammetric Engineering Remote Sens.*, **50**, 53.

Tucker, C.J., Townshend, J.R.G. and Goff, T.E., 1985a, African land-cover classification using satellite data. *Science*, **227**, 369-375.

Tucker, C.J., VanPraet, C.L. Sharman, M.J. and van Ittersum, G., 1985b, Satellite remote sensing of total herbaceous biomass production in the Senegalese Sahel: 1980-1984. *Remote Sens. Environ.*, **17**, 233-249.

Tucker, C.J., Fung, I.Y. Keeling, C.D. and Gammon, R.H., 1986a, The relationship of global green leaf biomass to atmospheric CO_2 concentrations. *Nature*, **319**, 159-199.

Tucker, C.J., Justice, C. O., and Prince, S. D., 1986b, Monitoring the grasslands of the Sahel 1984-1985. *Int. J. Remote Sens.*, **7**, 1571-1582.

Tucker C.J, and P.J. Sellers, 1986, Satellite Remote Sensing of Primary Production, *Int. J. Remote Sens.*, 1986, **7**, 1395-1416.

Tucker, C.J., Dregne, H.E. and Newcomb, W.W., 1994, AVHRR data sets for determination of desert spatial extent, *Int. J. Remote Sens.*, **15**, 3547-3565.

Tucker, C.J., H.E. Dregne, W.W Newcomb, 1991, Expansion and contraction of the Sahara desert from 1980-1990, *Science*, **253**, 299-301.

UNCOD, 1977, Desertification: Its Causes and Consequences. Secretariat of United Nations Conference on Desertification. Nairobi, Kenya, Pergamon Press.

Vermote, E.F., and Kaufman, Y.J., 1995, Absolute calibration of AVHRR visible and near-infrared channels using ocean and cloud views. *Int. J. Rem. Sens.*, **16**, 2317-2340.

Vermote, E.F., Tanre, D., Seuze, J.L., Herman M. and Morcrette, J.J., 1995, 6S user guide version 1. College Park, Maryland, Department of geography, University of Maryland,.

Vermote, E., El Saleous, N., Kaufman, Y. J. and Dutton, E., 1997. Data pre-processing: Stratospheric aerosol perturbing effect on the remote sensing of vegetation: Correction method for the composite NDVI after the Pinatubo Eruption. *Remote Sensing Reviews*, **15**. 7-21.

White, F., 1983, The vegetation of Africa. Natural Resources Research vol. XX, UNESCO, Paris.

Wilson, M.F., and Henderson-Sellers, A., 1985, A global archive of land cover and soils data for use in general circulation models. *J. Climatology*, **5**, 119-143.

Wilson, E.O., 1988. In: Wilson E.O. and Peters, F.M. (ed.)., *Biodiversity,* National Academy Press, Washington, DC, 1988.